

Research on a Novel Millimeter-wave Linear MEMS Array Antenna Based on Hadamard Matrix

Shu-yuan Shi, Yong-sheng Dai
Nanjing University of Science & Technology
No.200 Xiaolingwei, Nanjing, China
shuyuan_shi90@163.com

Abstract—In this paper, a new angular super-resolution technique called Phase Weighting Super-resolution Method (PWSM) based on Hadamard matrix is proposed, which is used in conventional phased array radar for improving angle resolution. The phase shifting necessary to steer the main beam of the aperture coupled micro-strip antenna is achieved by $0-\pi$ MEMS phase shifters, which are integrated in a hybrid fashion between the antenna and feed network. The results of the measured pattern are consistent with the theoretical calculation results.

I. INTRODUCTION

It is well known that the angle resolution is very important in some radar applications. In order to improve the angular resolution, we use an antenna with a large diameter, which leads to an increase in cost, volume, and wind resistance. Due to this reason angular super-resolution has gained a great concern. It can be applied to either element-space or beam-space observations. In the element space-estimations, there have appeared many Fourier transform-based algorithms beyond the conventional methods. Individual complex response can be obtained through the element-space estimation. In this paper, PWSM is a combination of the phase weighting method and the non-linear spectral estimated algorithm, and to realize the angular super-resolution for the conventional phased array radar, beam-space data are observed in [3] by using a Hadamard matrix as the beam-former matrix.

We design a double-layer aperture-coupled micro-strip antenna. Micro-strip antenna has quite a few advantages such as a lower profile, a smaller size and a lighter weight and so on. Double-layer aperture-coupled antenna with thick substrate can achieve a wideband. To obtain a large gain and achieve a specific directivity, an antenna array is often applied. Our antenna array utilizes an 8-element linear array with combination of the feed structure.

Recently, RF Micro-electro-mechanical system (MEMS) switch has drawn much attention due to its rapid isolation and connection, low insertion loss, low turn-on voltage, high reliability, as well as good performance of the reconfiguration in microelectronics, which is better than the PIN diode and MESFET switch. Based on MEMS switch, MEMS phase shifter, switch filter and switch array can be made and widely used in radar, satellite communications, wireless

communications and other systems, e.g. in the application of the antenna arrays shown in this paper.

II. ARCHITECTURE

A. Angular Super-resolution Based on Hadamard Matrix

In most of the conventional phased array radar, only the phase corresponding to each antenna element can be adjusted, i.e., only phase weighting can be applied. The discrete Fourier transform (DFT) beam-former matrix [1] or Hadamard beam-former matrix [4] is good candidate for the phase-only weighting. Alternatively, we choose Hadamard beam-former matrix. The coefficients of the Hadamard matrix are either $+1$ or -1 , so only 0° or 180° phase weightings are required.

In [3], to evaluate the performance of the proposed method, Monte Carlo simulation has been applied to estimate the root mean square error (RMSE) of the angle estimates and the spatial resolution SNR threshold in cases of either nonfluctuating targets or fluctuating targets. For an X band conventional phased array antenna with 139 elements, by using Phase Weighting Super-resolution Method (PWSM), the angular resolution is improved by a factor of 2 when SNR equals 15 dB. The PWSM can be applied in the design of new or conventional phased array radar systems. It is also possible to be applied in some communication systems. Fig. 1 shows the scheme of phased array antenna.

If the arriving signal deviates from the normal direction, the phase distribution will change quickly. Therefore we need the space intensive sampling. However, in the phased antenna array, it is easy to align scanning beam to the target. We use a space sparse sampling to reduce the number of phase weight statuses and accelerate the real-time processing speed. For example, after aligning the transmitting and receiving beam to the target of interest, we choose the appropriate value of M to form Hadamard matrix and realize the super-angle resolution. In this way, the number of phase weight statuses is reduced to half of the element number of the antenna array.

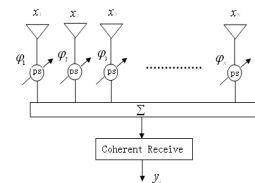


Fig.1. Scheme of phased array antenna.

B. The Design of Double-layer Aperture-coupled Micro-strip Antenna Array

Based on the requirement and the recent situation in relevant fields, we proposed the issue: millimeter-wave MEMS $0-\pi$ phased one-dimension 1×8 super-resolution array antenna, whose feed network, phase scanning, antenna array are respectively realized by micro-strip antenna array, micro-strip feeder, millimeter-wave MEMS and drive circuit. In this way we can use existing technique and qualification to realize super-resolution character by using millimeter MEMS vary the phase of $0-\pi$. The radiate implement utilizes micro-strip antenna unit and RT/5880 substrate, whose permittivity is 2.2. The input port utilizes W28 waveguide. The guide line is: center frequency at 35GHz, bandwidth larger than 5%, the largest gain better than 13dB when all units of array are at the same phase. One difficulty is the solution of the mutual coupling of the antenna array and the feed structure.

The three-dimensional analysis of aperture coupled micro-strip antenna is shown in Fig.2. It has a rectangle patch of size $a \times b$. The micro-strip patch fed by the micro-strip line through the aperture or the crack in common ground is also shown in Fig. 1. The aperture is with center of (x_0, y_0) and size of $L_a \times W_a$. The width of micro-strip line is W . The thickness of substrate is t .

In our design, we choose the double-layer media made of RT/5880 substrate with the thickness of 0.254 mm. There is an air gap of 0.5 mm thickness between the double media, which can be used to widen the wideband of our antenna. With the aid of IE3D, we get the patch length is 2.7mm and the width is 3.4mm. The coupling gap length is 2.4 mm and the width is 3.4 mm. The micro-strip feed is 0.73 mm beyond the center of gap, whose width is 0.78 mm. While debugging, we notice that coupling resistance reduces significantly as the width of patch increase, which indicates the gap coupling declines. The resonant frequency is sensitive to the length of patch. Generally gap length should not be too much long, otherwise back radiation will increase, but coupling cannot be ensured if it is too short. So, we must compromise while designing. The VSWR and the gain are shown in Fig. 3.

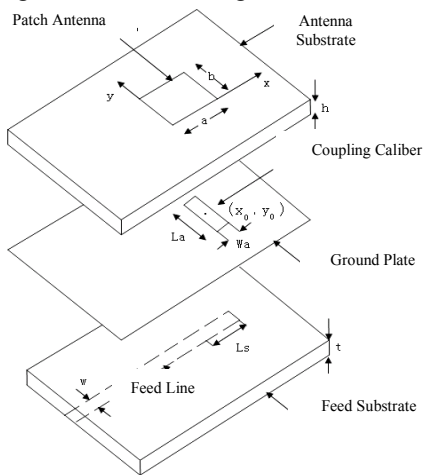


Fig. 2. Antenna model analysis.

To obtain a larger gain and achieve a specific directivity, the simplest way is a linear array. Due to the simple and compact feed network the transmission loss of series-fed array [5] is small. The combination of multiple series feed array can easily meet the beam required.

The antenna array is fed by one divide eight power divided network, in which the distance from feed source to every unit is all uniform. The distance between antenna unites is $0.8 \lambda_0$. The 1×8 coupling antenna array simulation block diagram is shown in Fig. 4. The simulation results of the antenna array are shown in Fig. 5.

We use a waveguide to micro-strip probe device to transform waveguide to micro-strip, which occupied a small space, the waveguide and micro-strip are orthogonal to each other. Too big waveguide hatch will arouse seriously leak and influence the pattern. While it is hard to be fixed and completely separate the waveguide from the micro-strip with too small waveguide patch, which will lead to short-circuit. Through the optimization, we get that the patch length is 1.6mm, the width is 0.66mm, and the distance from probe to jumper is 1.35mm. The feeding structure is shown in Fig. 6.

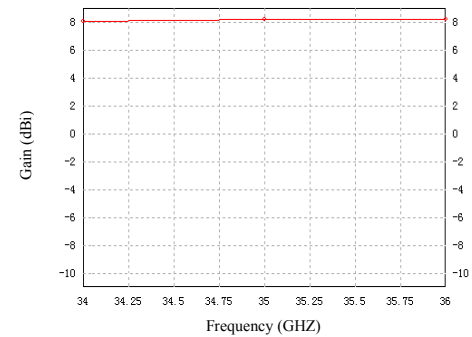
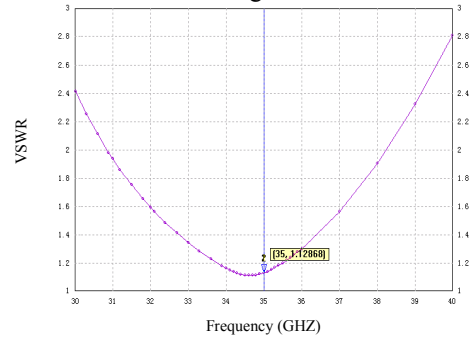


Fig. 3 VSWR and gain of the antenna.

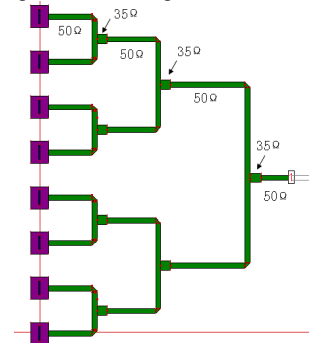


Fig. 4 Simulation block diagram of coupling antenna array.

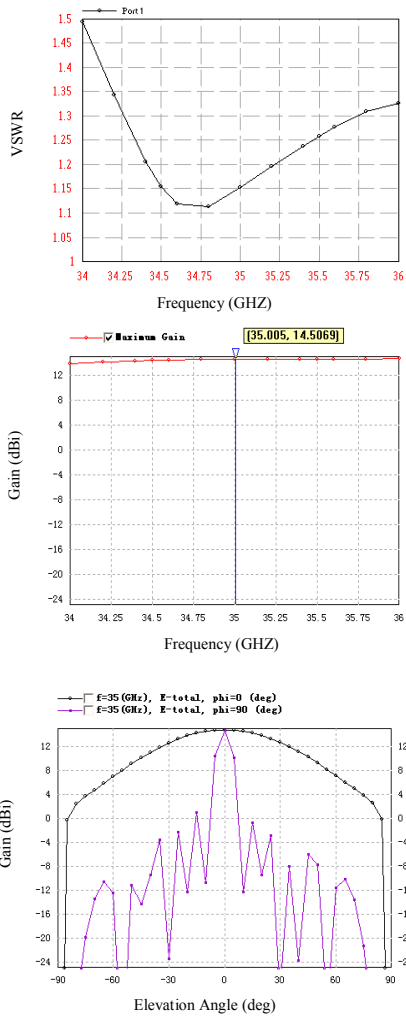


Fig. 5 Performance of the array antenna.

C. MESFET Switches

RF MEMS switch utilizes the electrostatic adsorption to control the cantilever's up and down to achieve the switch's on and off, and eliminates the PN junction in the semiconductor and metal-semiconductor junction in the RF device. We can control the MEMS switch by DC bias. The performances of switch such as insertion loss and isolation degree depend on the capacitance values of the on and off states. Table I shows the comparison with three types of switches.

Generally, in accordance with the contact manner, RF MEMS switch can be classified in two types: one is the capacitive coupling type [2] and the other is the metal contact type [6]. We establish both of their models in HFSS to discuss their principles and structures.

Metal contact MEMS switches work similarly to the capacitive coupling MEMS switches. By the driving of static electric we can control the metal cantilever's movements, thus realizing the circuit's on and off. The difference is a metal contact type MEMS switch is equivalent to a variable capacitance connected in series in the circuit.

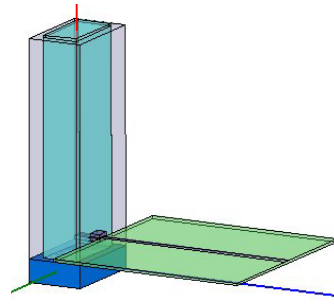


Fig. 6. Feed structure.

TABLE I
PROPERTIES SUMMARY OF THREE TYPES OF SWITCHING DEVICES

Type of switching devices	MEMS switches	PIN diodes	GaAs MESFET switches
Insertion loss	Excellent	Good	Good
Isolation degree	Excellent	Good	Good
Power capacity	Excellent	Good	Bad
Driving power	Excellent	Bad	Excellent
Switch speed	Bad	Good	Excellent
Cost	Good	Good	Bad

D. The Switched-line MEMS Phase Shifter

The phase shifter above is no longer applicable when the frequency rises to the millimeter wave band. The application of MEMS technology to the millimeter-wave phase shifter can greatly reduce size and weight, especially for aerospace weapons.

According to the analysis above, we need the phase shifter to realize the super angle resolution. We choose metal-contact cantilever MEMS series switch to control the $0-\pi$ phase shifter. As is shown in Fig. 7, the phase shifting $\Delta\phi$ is 179.88° to ensure that the signal into the antenna array is of equal amplitude and inverted.

The photo of physical metal-contact cantilever MEMS series switch is present in Fig. 8 (a). The switched-line MEMS phase shifter is present in Fig. 8 (b).

III. MEASUREMENT

The antenna array and phase shifter are both made by Nanjing 14 research institute. Antenna array and phase shifter are compatible for that they both utilize the same media. All metal patches are gilded to prevent them from oxidation. The final sample is shown in Fig. 9.

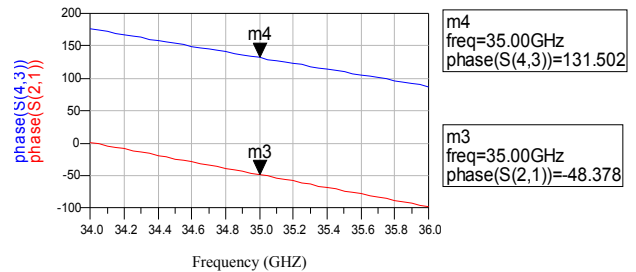


Fig. 7. Phase shifting of phase shifter.

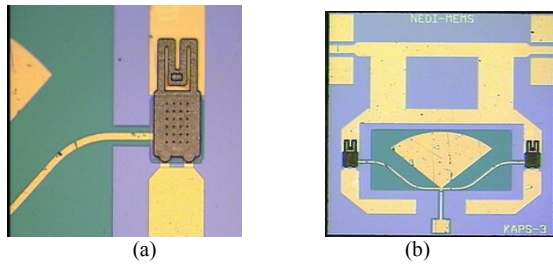


Fig. 8. Physical metal-contact cantilever MEMS switch and phase shifter. (a) MEMS switch. (b) MEMS phase shifter.

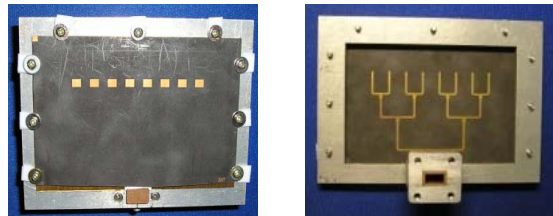
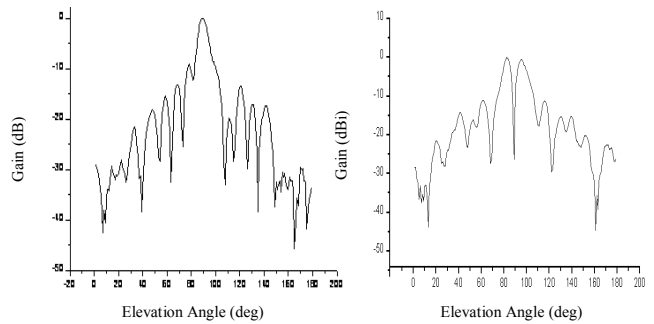
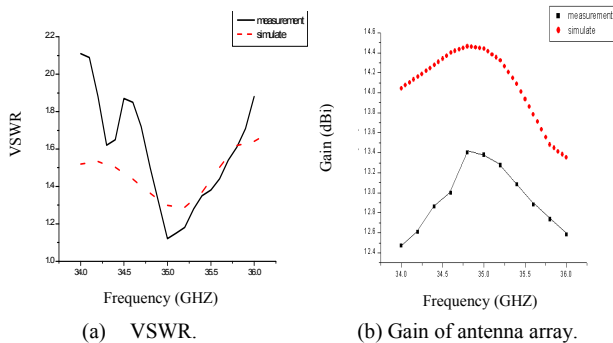


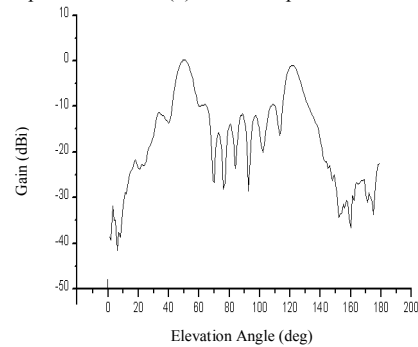
Fig. 9. Sample of antenna.

Simulate (dotted line) and measured (solid line) VSWR is shown in Fig. 10 (a). The simulated and measured gain of antenna array is shown in Fig. 10 (b). When eight antennas are all at the same shift phase of 0° , the measured pattern is shown in Fig. 10 (c). When shift phase of eight antennas are alternate with 0° and 180° , the measured pattern is shown in Fig. 10 (d). When the first four antennas are at the shift phase of 0° and the other antennas are at the shift phase of 180° , the measured pattern is shown in Fig. 10 (e). It can be seen that the results of the measured pattern are consistent with the theoretical calculation results. The join of the phase shifter in antenna array results in the small distance between the feed network and itself.

We chose a phase shifter online testing, i.e., by putting a phase shifter into a uniform antenna array and measuring a received signal's amplitude and phase distribution, we can estimate the amplitude and phase distribution of the caliber of the antenna according to the inverse change of Walsh-Hadamard matrix, then judge the working condition of the phase shifter. In millimeter wave band, especially when the phase shifter and the antenna array integrated together, a separate test of phase shifter is very difficult, so the method above is a valid and reliable one.



(c) Measured pattern at 0° . (d) Measured pattern at alternate 0° and 180° .



(e) Measured pattern at the shift phase of 0° in the first four antennas and 180° in the other antennas.

Fig. 10. Performance of measured pattern.

IV. CONCLUSIONS

In this work an 8×1 MEMS antenna array with phase shifter for 34.2GHz-36GHz has been designed. The VSWR of the antenna is better than 2. The non-inverting gain is better than 13 dB and the horizontal beam-width is 5.8° - 6.2° .

ACKNOWLEDGMENT

The authors are grateful to Nanjing University of Science & Technology.

REFERENCES

- [1] Zoltowski, M. D., Kautz, G. M., and Silverstein, S. D. 1993 Beamspace Root-MUSIC. *IEEE Transactions on Signal Processing*, 41, 1993, pp. 344-364.
- [2] C. Goldsmith, T. H. Lin, B. Powers, W. R. Wu, Norvell B, "Micromechanical membrane switches for microwave applications" *Tech. Digest, IEEE Microwave Theory and Techniques Symp*, 1995, pp.91-94.
- [3] W. X. Sheng, D. G. Fang, "Angle super-resolution for phased antenna by phase weighting", *IEEE Transactions on Aerospace and Electronic Systems*, 2001, VOL. 37, NO. 4.
- [4] Fang, D. G., Sun, J. T., Wang, Y., and Sheng, W. X. 1995. "Realization of radar cross-range resolution by array phase weighting," *Chinese Journal of Radio Science*, 10, 1995, pp. 1-3.
- [5] J. X. Yin, K. C. Liu, "Calculation of series-feed micro-strip antenna array's gain and pattern," *National University of Defense Technology*, Vol. 22, pp. 43-46.
- [6] J. J. Yao, M. F. Chang, "A surface micromachined miniature switch for telecommunications applications with signal frequencies from DC up to 4 GHz," *Tech. Digest, 8th Int. Conf. on Solid-State Sensors and Actuators*. 1995. pp. 384-387.